Two-time correlation functions of a harmonic system nonbilinearly coupled to a heat bath: Spontaneous Raman spectroscopy

K. Okumura and Y. Tanimura
Division of Theoretical Studies, Institute for Molecular Science, Myodaiji, Okazaki, Aichi 444, Japan
(Received 11 March 1997)

A harmonic system coupled to a heat bath comprised of harmonic oscillators through a nonbilinear system-bath interaction $q^2 q_j$ is considered, where q and q_j are the system and bath coordinates, respectively. The two-time correlation functions for the model are analytically obtained through a diagrammatic expansion. Numerical calculations of the analytical results are presented for the spontaneous (frequency-domain) Raman spectroscopy. Comparison with numerical results from the conventional linear-coupling model (the Brownian oscillator model) are made, which indicates experimentally distinguishable temperature dependences. [S1063-651X(97)08609-1]

PACS number(s): 05.70.−a, 31.15.−p, 33.20.Fb

In the Brownian oscillator model [1–3], the harmonic oscillator system is coupled to the heat bath consisting of an infinite number of harmonic oscillators. The coupling between the main system and the bath is assumed to be bilinear, i.e., qq_j. The Gaussian property is guaranteed for a bath consisting of harmonic oscillators bilinearly coupled to the main system. Although a number of experiments have been well explained by the Brownian model, one needs to modify the model to have a better description of realistic systems. Generalization to, for example, an anharmonic bath or nonbilinear coupling breaks the Gaussian nature of the noise produced by the Brownian bath.

As such an example, we consider in this article a system with square-linear coupling (the SL model) denoted by $q^2 q_j$ in terms of the two-time correlation function. Although the conventional linear-linear coupling (the LL model) causes dissipation in the system dynamics, it does not modulate the fundamental frequency ω_0 of the main harmonic system. If we assume the square-linear interaction, however, ω_0 will fluctuate as $\omega_0+\Omega(t)$, where $\Omega(t)$ is the noise produced by the bath. By use of the terminology of the reduced density matrix, the difference of the two models is that in the SL model the pure dephasing is the mechanism of dissipation, which is not included in the LL model.

The deviation from the Brownian system can be directly detected by optical measurements such as impulsive stimulated scattering (ISS), optical Kerr effect (OKE), and infrared absorption (IR), which are related to the antisymmetric time correlation function $\langle[q(t),q(0)]\rangle$ [3]. In this article, we calculate the correlation functions for the LL and the SL model, and then show how one can use the off-resonant Raman spectroscopy to distinguish the two models.

Besides the above-mentioned interests, the SL model is important in that it connects the stochastic model to the Brownian (or the LL) model. The stochastic model is based on the assumption that the environment causes a random modulation of the vibrational frequency, whereas the Brownian model is based on the assumption that the environment causes the friction of motion by way of the random force [see the fluctuation dissipation relation in Eq. (5) below], which is described by the Langevin equation. In the SL model, the frequency of the mode of the system itself is modulated by the environment as in the stochastic model, while its classical dynamics can be described by the Langevin-type equation as in the LL model. Thus the SL model makes it possible to bridge the gap between the stochastic model and the dynamical models (such as LL model) which are based on the Langevin-type equation derived from the Hamiltonian.

As the main tool, we use the Feynman rule on the unified-time path (UTP) [4–6]. To derive the real-time correlation function at a finite temperature, there are two well-known techniques: the Matsubara and Keldysh formalisms. The former requires subtle analytical continuation, which is only applicable to the correlation function of two-time variables, while the latter makes it hard to include the initial correlation. The advantage of the UTP formalism is that a multi-(real-)time real-time correlation function such as $\langle q(t)q(t')\cdots q(t'')\rangle$ can be obtained, *without* performing the delicate analytical continuation but *with* the initial correlation automatically taken into account.

Consider models described by the Hamiltonian

$$H=\frac{p^2}{2m_0}+\frac{m_0\omega_0^2}{2}q^2+\sum_{j=1}^{N}\left\{\frac{p_j^2}{2m_j}+\frac{m_j\omega_j^2}{2}\left[q_j-\frac{F_j(q)}{m_j\omega_j^2}\right]^2\right\}, \tag{1}$$

where p,q are the momentum and coordinate of the main system and p_j,q_j are those of the jth degree of freedom of the bath oscillators. In the linear-linear coupling model (the LL model), $F_j(q)$ is chosen to be $F_j(q)=c_j\,q$. In this study, we introduce the square-linear model (the SL model) in which $F_j(q)=g_j\,q^2/2$. Note here that, in the LL model, the Hamiltonian has the coupling term qq_j, while, in the SL model, it has the coupling term q^2q_j. In addition, the SL model has the anharmonic contribution $\lambda q^4/4!$ to the potential, while the LL model has the frequency shifting term (the counter term) $\Delta q^2/2$ [2,1], where $\lambda=\Sigma_j(3g_j^2/m_j\omega_j^2)$, $\Delta=\Sigma_j(c_j^2/\,m_j\omega_j^2)$. To elucidate the physical picture associated with these models, we present the Euler-Lagrange equa-

tion derived from the Hamiltonian (1). We found that, for any $F_j(q)$, the equation of motion reduces to the generalized Langevin equation:

$$m_0\frac{d^2q}{dt^2}+\frac{dV}{dq}+m_0\int_0^t dt'\,\gamma(t-t')\frac{dq}{dt'}=R(t), \tag{2}$$

where the damping kernel is given by

$$\gamma(t-t')=\sum_{j=1}^{N}\frac{\partial F_j(q(t))}{\partial q(t)}\frac{\cos\omega_j(t-t')}{m_0m_j\omega_j^2}\frac{\partial F_j(q(t'))}{\partial q(t')}. \tag{3}$$

It should be noticed that the term $\Delta q^2/2$ in the LL model and the term $\lambda q^4/4!$ in the SL model have been eliminated from the equation of motion after tracing over the bath degrees of freedom: the potential in the above equation is given by $V(q)=m_0\omega_0^2q^2/2$. $R(t)$ is the fluctuating force which satisfies the relations

$$\langle R(t)\rangle_I=0, \tag{4}$$

$$\langle R(t)R(t')\rangle_I=\gamma(t-t')m_0/\beta, \tag{5}$$

where the expectation is the classical phase-space average with the initial distribution $e^{-\beta H}$ at the inverse temperature $\beta=1/k_BT$. In the SL model the damping kernel is a function of the coordinate: $\gamma(t-t')=q(t)\,\eta_{\rm SL}(t-t')q(t')$, while in the LL model it does not depend on q: $\gamma(t-t')=\eta_{\rm LL}(t-t')$. In the following, we study a quantum dynamics of the system in the case of $\eta_{\rm LL}(t)=\eta_{\rm LL}\delta(t)$ or $\eta_{\rm SL}(t)=\eta_{\rm SL}\delta(t)$.

In the Feynman rule on UTP [5,6], we use four independent propagators,

$$D^{(-+)}(t,t')=-\theta(t-t')\langle q(0)q(t)-q(t)q(0)\rangle_0,$$

$$D^{(--)}(t,t')=\frac{1}{2}\langle q(0)q(t)+q(t)q(0)\rangle_0,$$

$$D^{(-3)}(t,\tau)=\langle q(0)q(t+i\tau)\rangle_0,$$

$$D^{(33)}(\tau,\tau')=\theta(\tau-\tau')\langle q(i\tau')q(i\tau)\rangle_0+\theta(\tau'-\tau)\langle q(i\tau)q(i\tau')\rangle_0,$$

where the expectation value is defined by the noninteracting Hamiltonian H_0 as

$$\langle q(0)q(t)\rangle_0={\rm Tr}e^{-\beta H_0}qe^{iH_0t/\hbar}qe^{-iH_0t/\hbar}/{\rm Tr}e^{-\beta H_0}. \tag{6}$$

The correlation functions for the interacting system, $D_c^{(lm)}$, are given by replacing the noninteracting Hamiltonian by the full Hamiltonian in the definitions of the bare correlation functions, $D^{(lm)}$. For example, $D_c^{(-3)}(t,\tau)=\langle q(0)q(t+i\tau)\rangle$, where the expectation value is defined by Eq. (6) with H_0 replaced by H.

We found that, in the Fourier-Laplace representation, all the full correlation functions can be expressed through a single function $f(x)$ of a complex variable x:

$$D_c^{(-+)}(z)=\frac{\hbar}{i}f(z), \tag{7}$$

$$D_c^{(--)}(z)=-\frac{1}{\beta}\sum_{n=-\infty}^{\infty}\frac{z}{\nu_n}\frac{1}{z-\nu_n}[f(z)-f(\nu_n)], \tag{8}$$

$$D_c^{(-3)}(z,n)=-\hbar\frac{1}{z-\nu_n}[f(z)-f(\nu_n)], \tag{9}$$

$$D_c^{(33)}(n)=\hbar f(\nu_n), \tag{10}$$

where $\nu_n=2\pi n/(\beta\hbar)$. To obtain the function $f(x)$, we derive $D_c^{(-+)}(z)$ through perturbative calculations. The diagrammatic expansion of $D_c^{(-+)}(z)$ is then calculated by using the Feynman rule as [5]

$$D_c^{(-+)}(z)=\frac{1}{[D^{(-+)}(z)]^{-1}-\Sigma(z)}, \tag{11}$$

where

$$D^{(-+)}(z)=\frac{\hbar}{i}\frac{1}{m_0}\frac{1}{\omega_0^2+z^2}. \tag{12}$$

In the LL model, the self-energy $\Sigma(z)$ is exactly given by $\Sigma(z)=-\eta_{\rm LL}z$ [5]. In the SL model the self-energy $\Sigma(z)$ is calculated up to the second order in g_j as

$$\Sigma(z)=\Sigma_a+\sum_{j=1}^{N}\left(\Sigma^j+\int_0^\infty dt\;e^{-zt}[\Sigma_d^j(t)+\Sigma_e^j(t)]\right), \tag{13}$$

where the sum $\Sigma^j\equiv\Sigma_b^j(t)+\Sigma_c^j(t)$ is time independent though each element $\Sigma_b^j(t)$ or $\Sigma_c^j(t)$ depends on time. Each term can be described by a diagram and analytical expressions for such diagrams are given by

$$\Sigma_a=-\frac{i}{2\hbar}\lambda D^{(--)}(0,0),$$

$$\Sigma_b^j(t)=\frac{i}{2\hbar^2}g_j^2D^{(33)}(0,0)\int_0^{\beta\hbar}d\tau D_j^{(-3)}(t,\tau),$$

$$\Sigma_c^j(t)=\frac{-1}{2\hbar^2}g_j^2D^{(--)}(0,0)\int_0^t dt'D_j^{(-+)}(t,t'),$$

$$\Sigma_d^j(t)=-\frac{1}{\hbar^2}g_j^2D_j^{(-+)}(t,0)D^{(--)}(t,0),$$

$$\Sigma_e^j(t)=-\frac{1}{\hbar^2}g_j^2D^{(-+)}(t,0)D_j^{(--)}(t,0).$$

Introducing the spectral density defined by

$$J(\omega)=\sum_{j=1}^{N}\frac{\pi g_j^2}{2m_j\omega_j}\delta(\omega-\omega_j), \tag{14}$$

the summation over j in Eq. (13) is replaced by the integral. If we assume $J(\omega)=m_0\eta_{\rm SL}\omega$, which is equivalent to setting $\eta_{\rm SL}(t)=m_0\eta_{\rm SL}\delta(t)$, this integration is divergent. To regular-

ize the divergent integral, we introduce a convergent factor $e^{i\varepsilon\omega}$, where ε is a positive small number and shall be set to zero at the end. To eliminate the divergence we replace the frequency ω_0^2 in the Hamiltonian Eq. (1) by $\omega_0^2+\Delta\omega_0^2$ where $\Delta\omega_0^2=(2\hbar\eta_{\rm SL}/\pi)\ln(1-e^{-\nu_1\varepsilon})$. After this renormalization, we have

$$\tilde{\Sigma}_R(z)=i\frac{\hbar\eta_{\rm SL}}{2m_0\omega_0^2}[S_1(z)+S_R(z)], \tag{15}$$

where

$$S_1(z)=\frac{iz}{\omega_0}\coth\frac{\beta\hbar\omega_0}{2}+\frac{iz-\omega_0}{2\omega_0}\coth\frac{iz-\omega_0}{2}\beta\hbar - \frac{iz+\omega_0}{2\omega_0}\coth\frac{iz+\omega_0}{2}\beta\hbar, \tag{16}$$

and

$$S_R(z)=\frac{4i}{\beta\hbar}\sum_{n=1}^{\infty}\frac{\nu_n^2(3z^2-\omega_0^2)-(\omega_0^2+z^2)^2}{\nu_n\{(\omega_0+iz)^2+\nu_n^2\}\{(\omega_0-iz)^2+\nu_n^2\}}. \tag{17}$$

From Eqs. (7) and (11) we finally obtain

$$f(x)=\frac{1}{m_0\omega_0^2}\frac{1}{(\omega_0^2+x^2)/\omega_0^2-\tilde{\Sigma}_R(x)}, \tag{18}$$

where $\tilde{\Sigma}_R(x)$ is defined through Eqs. (15)–(17). Combined with Eqs. (7)–(10), we now have analytical expressions for all the $D_c^{(lm)}$ within the present approximation since the function $f(x)$ is given by Eq. (18). In the case of the LL model, $f(x)$ is expressed in Eq. (18) by replacing $\tilde{\Sigma}_R(x)$ by $-\eta_{\rm LL}x/\omega_0^2$.

Within the linear approximation of the polarizability ($\alpha=\alpha_0+\alpha_1 q$), the (off-resonant) spontaneous Raman signal is given by [3]

$$I(\omega)=2\alpha_1^2{\rm Re}\int_0^{\infty}dt\langle q(0)q(t)\rangle e^{i\omega t}, \tag{19}$$

where ω is the Raman shift. We thus have

$$I(\omega)={\rm Re}\left[\frac{1}{\beta\hbar}\sum_{n=-\infty}^{\infty}e^{i\nu_n 0^+}h_n\right], \tag{20}$$

where $h_n=D_c^{(-3)}(i\omega,n)$. Here $D_c^{(-3)}(i\omega,n)$ is defined by Eq. (9) in which $f(x)$ is now given by Eq. (18) for the SL model. The results for the LL model can also be obtained by replacing $\tilde{\Sigma}_R(x)$ in Eq. (18) by $-\eta_{\rm LL}x$. Here, 0^+ is an infinitesimally small positive quantity. Note here that the convergence factor $e^{i\nu_n 0^+}$ plays an important role since $h_n\sim 1/|n|$ at large n. We rewrite the above expression to improve the convergence of the summation over n for numerical estimations:

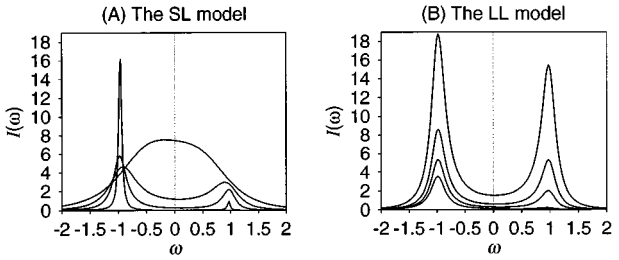

FIG. 1. The temperature dependence of Raman line shape for (A) the SL model with $\tilde{\eta}_{\rm SL}=0.3$ and (B) the LL model with $\tilde{\eta}_{\rm LL}=0.3$. The intensity $I(\omega)$ in the figure and the other variables are dimensionless as defined below Eq. (22). The solid line from the lowest to the highest one around $\tilde{\omega}=0$ corresponds to the inverse temperatures (a) $\tilde{\beta}=3.0$, (b) $\tilde{\beta}=1.0$, (c) $\tilde{\beta}=0.5$, and (d) $\tilde{\beta}=0.2$, respectively. If we set $\omega_0=210\ {\rm cm}^{-1}$, the temperatures are (a) 100 K, (b) 300 K, (c) 600 K, (d) 1500 K.

$$I(\omega)={\rm Re}\left[\frac{i}{2}\hbar f(i\omega)+\frac{1}{\beta\hbar}h_0+\frac{1}{\beta\hbar}{\sum_{n=-\infty}^{\infty}}'\left(h_n-\frac{\hbar f(i\omega)}{\nu_n}\right)\right], \tag{21}$$

where Σ' implies that the summation does not include $n=0$. In the following, numerical calculations are carried out using Eq. (21) for both models.

In the high temperature limit $\beta\to 0$, Eq. (21) reduces to

$$\tilde{I}(\omega)\to\frac{1}{\tilde{\beta}}\frac{\tilde{\eta}_{\rm eff}}{(\tilde{\omega}_0^2-\tilde{\omega}^2)^2+(\tilde{\omega}\tilde{\eta}_{\rm eff})^2}, \tag{22}$$

where $\tilde{\eta}_{\rm eff}=\tilde{\eta}_{\rm LL}$ $(=\tilde{\eta}_{\rm SL}/\tilde{\beta})$ in the LL (SL) model. Here we have used the dimensionless parameters defined as $\tilde{I}(\omega)=m_0\omega_0^2 I(\omega)/\hbar$, $\tilde{\eta}_{\rm LL}=\eta_{\rm LL}/\omega_0$, $\tilde{\eta}_{\rm SL}=\hbar\eta_{\rm SL}/(m_0\omega_0^2)$, $\tilde{\beta}=\beta\hbar\omega_0$, $\tilde{\omega}=\omega/\omega_0$, $\tilde{\omega}_0=\omega_0/\omega_0=1$.

Figure 1 compares the Raman spectra for various temperatures in the cases of (A) the SL model and (B) the LL model. We chose the system-bath coupling $\tilde{\eta}_{\rm LL}, \tilde{\eta}_{\rm SL}=0.3$, which satisfies the perturbative condition $\tilde{\eta}_{\rm LL}, \tilde{\eta}_{\rm SL}\ll 1$. At low temperature the Stokes ($\tilde{\omega}\sim -1$) and anti-Stokes ($\tilde{\omega}\sim 1$) lines are observed in both models. Since we assumed the linear polarization, $\alpha=\alpha_0+\alpha_1 q$, the scattered light originated from the transition between the jth and the $j\pm 1$th vibrational states. At low temperatures, the Stokes line mainly corresponds to the transition from the ground vibrational state $|0\rangle$ to the first excited state $|1\rangle$ while the anti-Stokes corresponds to the opposite process $|1\rangle\to|0\rangle$. The intensity of the Stokes line is larger than that of the anti-Stokes, since the initial population of the ground state $|0\rangle$ is larger than that of the first excited state $|1\rangle$. As the temperature increases, the relative strength of the anti-Stokes line increases since the initial population of excited states such as $|1\rangle$ and $|2\rangle$ increase. At higher temperature, the processes $|1\rangle\to|2\rangle$, $|2\rangle\to|3\rangle$, etc. ($|2\rangle\to|1\rangle$, $|3\rangle\to|2\rangle$, etc.) may contribute to the formation of the Stokes (anti-Stokes) line. The general features of the LL and SL models are similar, partially because the system-bath interactions are weak and the bath plays a minor role. The temperature dependences of the signal of the two models are, however, rather different. The

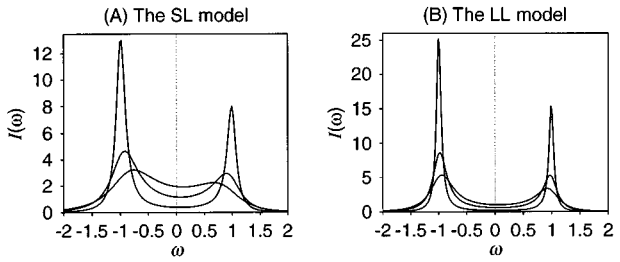

FIG. 2. The dependence of Raman line shape for the damping factors $\tilde{\eta}_{\mathrm{SL}}$, $\tilde{\eta}_{\mathrm{LL}}$ for (A) the SL model and (B) the LL model. Here, $\tilde{\beta}=0.5$. The solid line from the highest to lowest one around $\tilde{\omega}=0$ corresponds to (a) $\tilde{\eta}=0.5$, (b) $\tilde{\eta}=0.3$, and (c) $\tilde{\eta}=0.1$, respectively.

difference can be summarized by two points. (i) The signals of the two models for $\tilde{\eta}_{\mathrm{SL}}=\tilde{\eta}_{\mathrm{LL}}$ $(=0.3)$ are similar around $\tilde{\beta}=1$ and become different as $\tilde{\beta}$ deviates from one. (ii) At very high temperature, the two (Stokes and anti-Stokes) peaks merge to form a single central peak in the SL model while they remain separated in the LL model.

The reason for (i) is explained by Eq. (22) since the signals for the two models coincide with each other if we invoke Eq. (22) and set $\tilde{\beta}=1$.

The reason for (ii) is also explained by Eq. (22). At the highest temperature $\tilde{\beta}=0.2$, the limit expression (22) is well fit by the numerically calculated signals and the spectra for the LL and SL models can be expressed by the same expression with $\tilde{\eta}_{\mathrm{eff}}=\tilde{\eta}_{\mathrm{LL}}$ and $\tilde{\eta}_{\mathrm{eff}}=\tilde{\eta}_{\mathrm{SL}}/\tilde{\beta}$, respectively. This implies that the SL model at high temperatures behaves like a strongly damped LL model. Since Eq. (22) peaks at around $\omega=0$ for large $\tilde{\eta}_{\mathrm{eff}}$, a single peak is observed in the SL model as mentioned in (ii).

Figure 2 illustrates the signals for various coupling strengths $\tilde{\eta}_{\mathrm{SL}}$ and $\tilde{\eta}_{\mathrm{LL}}$ at the temperature $\tilde{\beta}=0.5$. The two (Stokes and anti-Stokes) peaks are broadened and shifted to $\omega=0$ for both models as the damping factors increase, which is in accord with the general experimental facts. The SL model, however, is more sensitive to the change of the damping constant than the LL model. This is again explained by the limit expression (22) if we remember that $\tilde{\eta}_{\mathrm{eff}}=\tilde{\eta}_{\mathrm{LL}}$ or $\tilde{\eta}_{\mathrm{SL}}/\tilde{\beta}$.

In conclusion, we successfully demonstrated that the square-linear coupling mechanism can be an interesting extension of the Brownian oscillator model for the description of a dissipative system. As clear from the numerical results, the two models, the SL model and LL model, may be distinguishable through the Raman spectroscopy or other $\langle q(t)q(0)\rangle$ experiments such as ISS and OKE. Recently, the higher-order optical processes related to $\langle q(t_n)q(t_{n-1})\cdots q(0)\rangle$ $(n>1)$ have been a subject of great interest [7,8,6]. If the system is Brownian, which produces Gaussian noise, all characteristics can be determined by the two-time correlation functions $\langle q(t)q(0)\rangle$, whereas, if the system deviates from Brownian, such higher-order optical processes can provide additional information. For example, Loring and Mukamel had developed the seventh-order Raman echo theory [7] analogous to the photon echo theory by applying the stochastic two-level model to the ground and the first excited vibrational states to study the inhomogeneous distribution of vibrational frequencies. Since their theory is based on the stochastic two-level model, which is a special case of the spin-boson model [9], one cannot apply their theory to the low frequency modes of liquids where the Brownian model has been successfully used. For instance, we cannot obtain such an echolike signal from the seventh-order Raman processes in the Brownian theory, since the vibrational frequencies are not fluctuating in this model. If we employ the square-linear coupling, however, the fundamental frequency of the main harmonic system will fluctuate and we can expect to have such an echo signal. Thus, by generalizing the Brownian system to the square-linear coupling, one can expect to establish a bridge between the Brownian motion theory and the stochastic or the spin-boson theory. We leave this problem of the higher-order optical processes in the SL model for a future study.

One of the authors (K.O.) thanks Dr. Keisuke Tominaga and Dr. Yoko Suzuki for informative discussions, and acknowledges Professor Rob Coalson for a critical reading of the manuscript.

[1] H. Grabert, P. Schramm, and G-L. Ingold, Phys. Rep. **168**, 115 (1988).

[2] A. O. Caldeira and A. J. Leggett, Ann. Phys. (N.Y.) **149**, 374 (1983); **153**, 445(E) (1984).

[3] S. Mukamel, *Principles of Nonlinear Optical Spectroscopy* (Oxford University Press, New York 1995).

[4] R. Fukuda, M. Sumino, and K. Nomoto, Phys. Rev. A **45**, 3559 (1992); K. Okumura and Y. Tanimura, Phys. Rev. E **53**, 214 (1996).

[5] K. Okumura and Y. Tanimura, J. Chem. Phys. **105**, 7294 (1996).

[6] K. Okumura and Y. Tanimura, J. Chem. Phys. (to be published); **106**, 1687 (1997).

[7] R. Loring and S. Mukamel, J. Chem. Phys. **83**, 2116 (1985); D. Vanden Bout, L. J. Muller, and M. Berg, Phys. Rev. Lett. **67**, 3700 (1991); R. Inaba, K. Tominaga, M. Tasumi, K. A. Nelson, and K. Yoshihara, Chem. Phys. Lett. **211**, 183 (1993).

[8] Y. Tanimura and S. Mukamel, J. Chem. Phys. **99**, 9496 (1993); K. Tominaga and K. Yoshihara, Phys. Rev. Lett. **74**, 3061 (1995); T. Steffen and K. Duppen, *ibid.* **76**, 1224 (1996); A. Tokmakoff and G. R. Fleming, J. Chem. Phys. **106**, 2569 (1997).

[9] Y. Tanimura and R. Kubo, J. Phys. Soc. Jpn. **58**, 101 (1989).